Simulation Studies of Shock Formation due to Interactions of Two Plasmas in a Magnetic Field and Modified Two-Stream Instabilities*)

Tatsunori URAGAMI and Mieko TOIDA

Department of Physics, Nagoya University, Nagoya 464-8602, Japan

(Received 26 November 2013 / Accepted 28 February 2014)

Shock formation due to interactions between exploding and surrounding plasmas and evolution of modified two-stream instabilities are studied using two-dimensional (2D) electromagnetic particle simulations. After the exploding ions penetrate the surrounding plasma, a strong magnetic-field pulse forms near the front of the exploding plasma. Because of modified two-stream instabilities, electromagnetic fluctuations grow to large amplitudes in this pulse. At $\Omega_i t \simeq 1$, where Ω_i is the ion cyclotron frequency, the pulse starts to reflect ions and to split into two pulses, which then develop into forward and reverse shock waves. For various values of the initial exploding plasma velocity and of the angle between the velocity and external magnetic field, 2D simulations are performed. The parametric dependence of the properties of the generated pulses and of magnetic fluctuations is discussed.

© *2014 The Japan Society of Plasma Science and Nuclear Fusion Research*

Keywords: collisionless shock, modified two-stream instability, whistler wave, particle simulation

DOI: 10.1585/pfr.9.3401035

1. Introduction

Strong disturbances, such as solar flares and supernova explosions, can generate shock waves via interactions between exploding and surrounding plasmas. When the plasmas are collisionless, shock formation processes are complex and are strongly influenced by the presence of an external magnetic field [1, 2]. In Ref. [3], the interactions between exploding and surrounding plasmas in an external magnetic field have been studied using theory and simulations for the case in which the initial velocity of the exploding plasma $\boldsymbol{v}_0$ is perpendicular to the external magnetic field $\boldsymbol{B}_0$. The shock formation processes were the following. After the exploding ions penetrate into the surrounding plasma, the exploding ions induce an electric field in the direction $-\boldsymbol{v}_0 \times \boldsymbol{B}_0$, which accelerates the surrounding ions in this direction. Then, the directions of the ion velocities significantly change because of the magnetic force, and a strong magnetic-field pulse forms near the front of the exploding ions. This pulse reflects the surrounding ions forward and exploding ions backward, which causes the splitting of the pulse into two pulses going forward and backward. These pulses subsequently develop into forward and reverse shock waves.

The above mentioned theoretical and simulation approaches were one-dimensional (1D). Recently, using two-dimensional (2D) electromagnetic particle simulations, we confirmed that essentially the same phenomena as in the 1D simulations occur in the 2D simulation for a case in which $\boldsymbol{v}_0$ is perpendicular to $\boldsymbol{B}_0$ [4]. Furthermore, we have investigated the evolution of modified two-stream instabilities, which were not included in 1D simulations. In this study, we also investigated the interactions between exploding and surrounding plasmas using 2D simulations. After describing the evolution of the magnetic field for a case of $\boldsymbol{v}_0$ being perpendicular to $\boldsymbol{B}_0$, we discuss the simulation results for various values of v_0 and θ, where θ is the angle between $\boldsymbol{B}_0$ and $\boldsymbol{v}_0$.

2. Simulation Model and Parameters

We use a 2D (two spatial coordinates and three velocity components) relativistic electromagnetic particle code with full ion and electron dynamics. A uniform external magnetic field is in the (x, z) plane, $\boldsymbol{B}_0 = (B_0 \cos\theta, 0, B_0 \sin\theta)$. The simulation plane is (x, z) with a size $L_x \times L_z = 8192\Delta_g \times 512\Delta_g$, where Δ_g is the grid spacing. The system is periodic in the z direction and is bounded in the x direction. The total number of simulation particles is $N \simeq 1.1 \times 10^9$.

As initial condition, we used an exploding plasma with fluid velocity $\boldsymbol{v}_0 = (v_0, 0, 0)$ in the region $x < b$ and a surrounding plasma at rest in the region $x > b$. This boundary is set $b = 3300\Delta_g$. The initial density ratio of exploding to surrounding plasmas is $n_{E0}/n_{S0} = 2$. The ion-to-electron mass ratio is $m_i/m_e = 200$. The light speed is $c/(\omega_{pe}\Delta_g) = 4.0$, and the electron and ion thermal velocities in the upstream region are $v_{Te}/(\omega_{pe}\Delta_g) = 0.5$ and $v_{Ti}/(\omega_{pe}\Delta_g) = 0.035$, respectively, where ω_{pe} is the

author's e-mail: toida@cc.nagoya-u.ac.jp

*) This article is based on the presentation at the 23rd International Toki Conference (ITC23).

© 2014 The Japan Society of Plasma Science and Nuclear Fusion Research

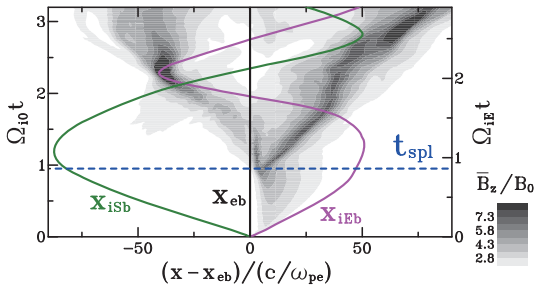

Fig. 1 Contour map of $\bar{B}_z(x,t)$ in the (x,t) plane and trajectories of ions and electrons that were initially at $x = b$, for $\theta = 90°$ and $v_0/v_A = 12$.

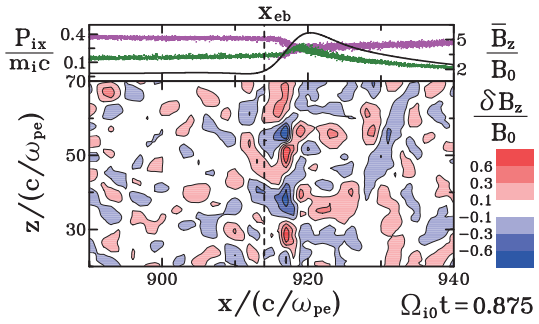

Fig. 2 Ion phase-space plots, x profile of $\bar{B}_z(x)$, and contour maps of $\delta B_z (= B_z - \bar{B}_z)$ in the (x,z) plane, at $\Omega_{i0}t = 0.875$.

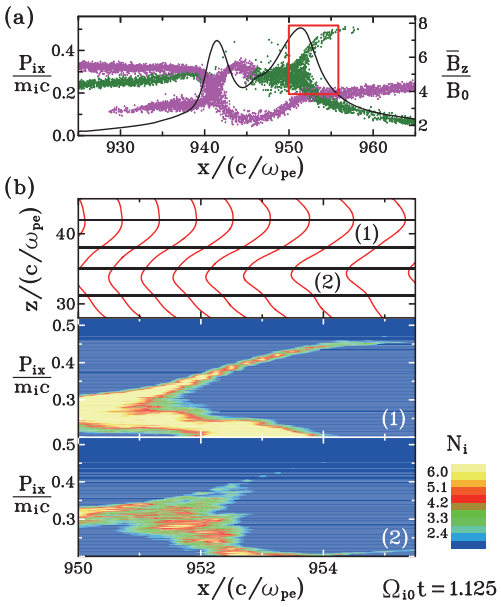

Fig. 3 (a) Ion phase-space plot and profile of $\bar{B}_z$ at $\Omega_{i0}t = 1.125$. (b) Expanded view of the front of the right pulse region enclosed by the red line in (a). Magnetic-field lines in the (x,z) plane and ion distributions for different ranges of z, (1) $38 < z/(c/\omega_{pe}) < 42$ and (2) $31 < z/(c/\omega_{pe}) < 35$.

electron plasma frequency averaged over the entire region. The magnetic field strength is $|\Omega_e|/\omega_{pe} = 0.5$; hence the Alfvén speed is $v_A/(\omega_{pe}\Delta_g) = 0.14$. We consider cases for $v_0/v_A < (m_i/m_e)^{1/2}$, for which the modified two-stream instabilities are more unstable than the ion Weibel instabilities [4].

3. Evolution of Magnetic Field

We briefly describe the evolution of magnetic field due to interactions between exploding and surrounding plasmas using data for $\theta = 90°$ and $v_0/v_A = 12$. Figure 1 shows the contour map of $\bar{B}_z(x,t)$ in the (x,t) plane, where $\bar{B}_z$ is the z-averaged B_z defined as

$$\bar{B}_z(x,t) = \frac{1}{L_z}\int dz B_z(x,z,t). \quad (1)$$

x_{iEb} (pink line) is the averaged trajectory of ions that were initially at the front of the exploding plasma, while x_{iSb} (green line) is for ions that were at the end of the surrounding plasma. Exploding and surrounding electrons do not mix because they move with $\boldsymbol{E}\times\boldsymbol{B}$ drift [3]. Their boundary is denoted by x_{eb}. The time in the left and right axes is normalized to Ω_{i0} and Ω_{iE}, respectively. Ω_{i0} is the cyclotron frequency of the surrounding ions in the upstream region, while Ω_{iE} is that of the exploding ions with initial speed v_0, which is defined as

$$\Omega_{iE} = \Omega_{i0}(1 - v_0^2/c^2)^{1/2}. \quad (2)$$

In the early stage $\Omega_{i0}t < 1$, the exploding ions penetrate the surrounding ions and are decelerated because of the $\boldsymbol{v}\times\boldsymbol{B}$ force. This intensifies $\bar{B}_z$ in the region $x_{eb} < x < x_{iEb}$, and a strong magnetic-field pulse is formed. At $t = t_{spl}$, which is shown by the horizontal dashed line, this pulse splits into two pulses, which then develop into shock waves, one propagating forward in the surrounding plasma away from x_{eb} and the other backward in the exploding plasma. This splitting is caused by ion reflection.

We now consider the 2D structure of B_z. In the region $x_{iSb} < x < x_{iEb}$ where exploding and surrounding ions overlap, relative cross-field motion between ions and electrons can excite modified two-stream instabilities through interactions with whistler waves [5–7]. The instabilities evolve in the magnetic field that is being gradually compressed. Because of the nonlinear evolution of the instabilities, 2D fluctuations grow to large amplitudes in the strong magnetic-field pulse region [4]. Figure 2 shows phase-space plots (x, p_{ix}) of surrounding ions (green dots) and exploding ions (pink dots), the x profiles of $\bar{B}_z$ and the contour maps of the 2D fluctuation of B_z, $\delta B_z = B_z - \bar{B}_z$, in the (x,z) plane at $\Omega_{i0}t = 0.875$, which is slightly before $t = t_{spl}$. The amplitudes of δB_z are noticeably large near the position where $\bar{B}_z$ has a steep slope and strong current is flowing.

The 2D fluctuations of the electromagnetic fields influence the ion reflection. Figure 3 (a) shows the ion phase space plot and the profile of $\bar{B}_z$ at $\Omega_{i0}t = 1.125$. Because ion reflection has already started, there are two pulses. The surrounding ions in front of the right pulse

with $p_{ix} > 0.3m_ic$ are reflected forward, which produced the right pulse. The exploding ions behind the left pulse with $p_{ix} < 0.2m_ic$ are reflected backward, which produced the left pulse. Figure 3 (b) displays an expanded view of the front of the right pulse region enclosed by the red line in Fig. 3 (a). The middle and bottom panels show ion distributions for the different range of z, $38 < z/(c/\omega_{pe}) < 42$ denoted by (1) and $31 < z/(c/\omega_{pe}) < 35$ denoted by (2). The ion reflection is strong in the z range (1), whereas it is weak in the z range (2). The top panel displays magnetic-field lines in the (x, z) plane. Magnetic-field lines bend forward in range (1) compared to range (2).

The evolution of 2D magnetic fluctuations after $t = t_{spl}$ is rather complex. This is because, in addition to the complex interactions between surrounding and exploding plasmas, the reflected ions can affect the field structure.

4. Dependence on v_0 and θ

We compare the results for the cases of $v_0/v_A = 12$ and 8. Figure 4 displays the contour map of $\bar{B}_z$ in the (x, t) plane for $v_0/v_A = 8$. A strong magnetic-field pulse splits into two at $\Omega_{i0}t_{spl} = 0.85$, which is earlier than the time for $v_0/v_A = 12$, $\Omega_{i0}t_{spl} = 0.95$. However, the values of $\Omega_{iE}t_{spl}$ for the two cases are close. The propagation speeds of the generated forward and reverse pulses for $v_0/v_A = 8$ are smaller than those for $v_0/v_A = 12$, respectively.

Figure 5 (a) shows the evolution of 2D fluctuations of B_z before $t = t_{spl}$ for $v_0/v_A = 8$ and 12. The contour maps of $|\overline{\delta B_z}|$ in the (x, t) plane are plotted. $|\overline{\delta B_z}|$ is defined as

$$|\overline{\delta B_z}|(x,t) = \frac{1}{L_z}\int dz|B_z(x,z,t) - \bar{B}_z(x,t)|, \qquad (3)$$

and the white line shows the position x_m where $\bar{B}_z$ has its peak value. The 2D fluctuations have large amplitudes in the region $x_{eb} < x < x_m$; the values of $|\overline{\delta B_z}|$ for $v_0/v_A = 8$ are smaller than those for $v_0/v_A = 12$. Figure 5 (b) shows the time variations of wavenumber k_z for the dominant modes of δB_z. At $\Omega_{i0}t \simeq 0.4$, k_z for $v_0/v_A = 8$ is slightly greater than that for $v_0/v_A = 12$, which is consistent with linear theory for modified two-stream instabilities. As time advances, k_z decreases. This is due to the nonlinear interactions of the current filaments produced by the instabilities [4]. The values of k_z for the two v_0's are close at $t \simeq t_{spl}$ for each v_0.

Figure 6 shows the evolution of δB_z after $t = t_{spl}$ for the two v_0's. The comparison of Fig. 6 (a) with Figs. 1 and 4 confirms that the amplitudes of δB_z are large in the forward- and reverse-pulse regions. The time variations of wavenumber k_z of the dominant modes in the two regions are shown in Fig. 6 (b). This indicates that k_z's start to decrease at $\Omega_{i0}t \simeq 2$ for the two v_0's, although there are some fluctuations. This time is almost equal to the time at which x_{iEb} and x_{iSb} intersect, as shown in Figs. 1 and 4.

In addition to $v_0/v_A = 8$ and 12, we performed simulations for $v_0/v_A = 10$, 14, and 16 at fixed $\theta = 90°$. Figure 7 (a) shows $\Omega_{iE}t_{spl}$ (black x-mark) as a function of v_0.

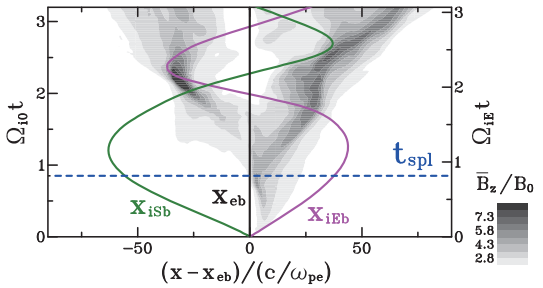

Fig. 4 Same as Fig. 1 except for $v_0/v_A = 8$.

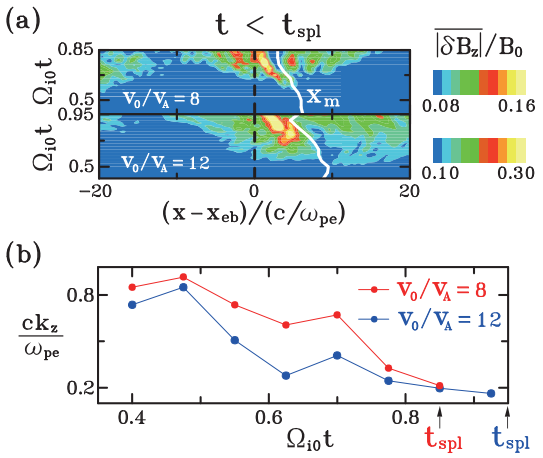

Fig. 5 Evolution of δB_z before $t = t_{spl}$ for $v_0/v_A = 8$ and 12. (a) Contour maps of $|\overline{\delta B_z}|$ in the (x, t) plane. (b) Time variations of wavenumber k_z of dominant mode.

We see that $\Omega_{iE}t_{spl} \sim 0.8$ for all v_0's. Figure 7 (a) also shows the Mach number $M_{fm}(\equiv |v_{sh}/v_{fm}|)$ of the generated forward (red square) and reverse (blue circle) shock waves from $\Omega_{i0}t = 2$ to 4, where v_{sh} is the propagation speed of a shock wave relative to x_{eb} and v_{fm} is the speed of fast magnetosonic waves in the upstream region of each shock wave. As v_0 increases, the M_{fm} values of the forward and reverse shock waves also increase.

We plot in Fig. 7 (b) the amplitude of $\bar{B}_z$, denoted by B_m, of a strong magnetic field pulse at $t = t_{spl}$ (black x-mark). The amplitudes of the generated forward and reverse shock waves are also shown; these are values averaged over the period from $t = 2/\Omega_{i0}(> t_{spl})$ to $4/\Omega_{i0}$. The values of B_m increase with v_0. We also show in Fig. 7 (c) the magnitude of 2D magnetic fluctuations in a strong magnetic-field pulse at $t = t_{spl}$, where σ_B is defined by

$$\sigma_B = \frac{1}{\Delta_x L_z}\int_{x_{min}}^{x_{max}} dx \int_0^{L_z} dz|\boldsymbol{B}(x,z) - \bar{\boldsymbol{B}}(x)|, \qquad (4)$$

where $\Delta_x = x_{max} - x_{min}$, $x_{min} = x_p - 25c/\omega_{pe}$ and $x_{max} = x_p + 25c/\omega_{pe}$ with x_p being the position of the pulse. The value of σ_B is normalized by B_m. As for 2D fluctuations in the generated forward and reverse shock waves, the time averaged values of σ_B/B_m are shown in Fig. 7 (c). The ratio σ_B/B_m gradually increases with v_0. The val-

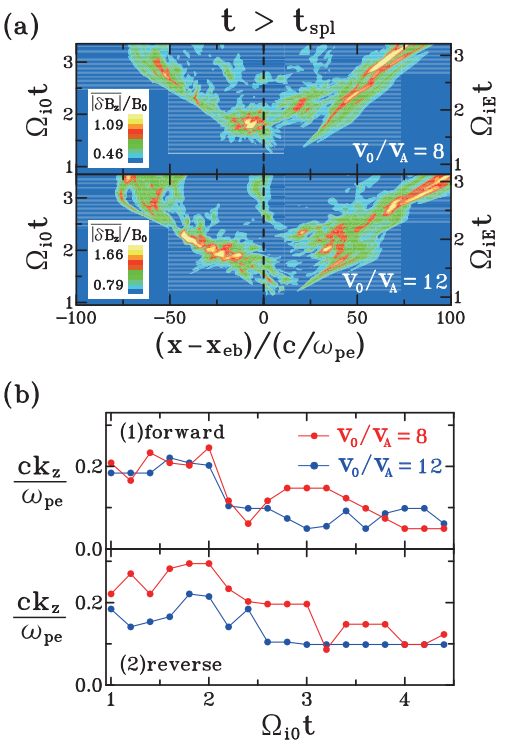

Fig. 6 Evolution of δB_z after $t = t_{\rm spl}$ for $v_0/v_{\rm A} = 8$ and 12. (a) Contour maps of $|\overline{\delta B_z}|$. (b) Time variations of k_z of dominant mode in the forward pulse region (1) and reverse pulse region (2).

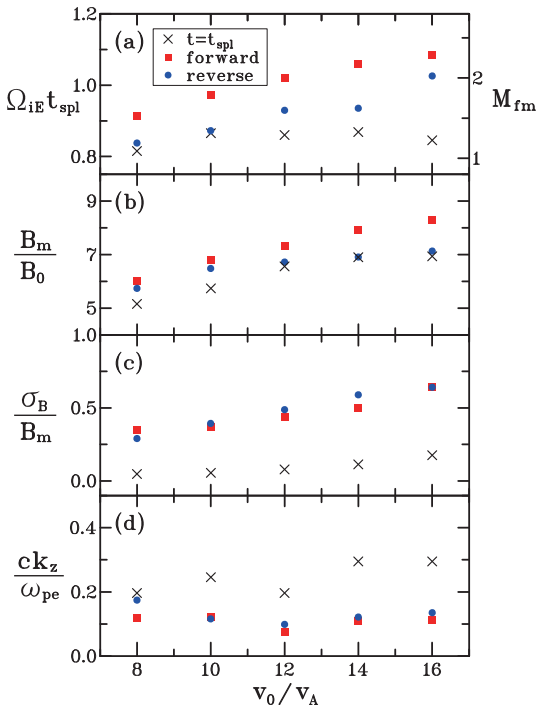

Fig. 7 Dependence on v_0. (a) Time $t_{\rm spl}$ (black x-mark). Mach number $M_{\rm fm}$'s of the forward (red square) and reverse (blue circle) shock waves from $\Omega_{\rm i0}t = 2$ to 4. (b)-(d) The values of $B_{\rm m}$, $\sigma_{\rm B}$, and k_z of the dominant mode of δB_z at $t = t_{\rm spl}$ (black x-mark) and their averaged values from $\Omega_{\rm i0}t = 2$ to 4 in the forward (red square) and reverse (blue circle) shock waves.

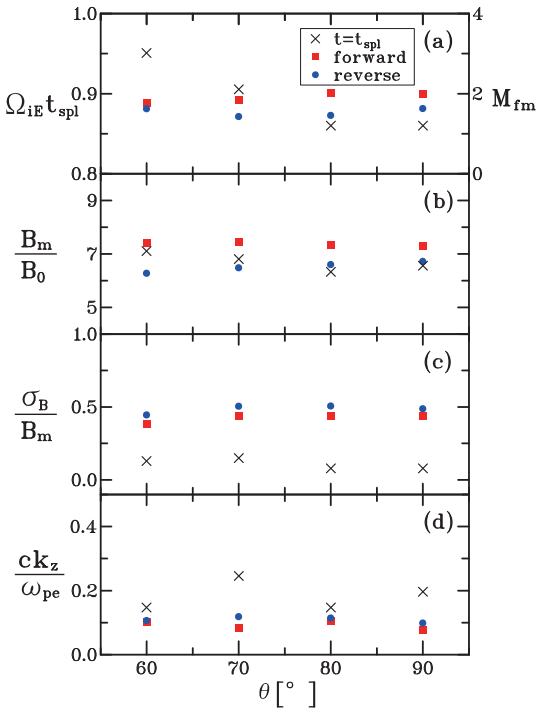

Fig. 8 Dependence on θ. Same as Fig. 7 except that x-axis is θ.

ues of $\sigma_{\rm B}/B_{\rm m}$ in the forward and reverse shock waves are greater than that in the strong magnetic-field pulse. Figure 7 (d) shows the wavenumber k_z of the dominant mode of δB_z. Compared to k_z of the strong magnetic-field pulse at $t = t_{\rm spl}$, k_z's of the forward and reverse shock waves are small. The dependence of k_z on v_0 is not so clear.

We next present the results for $\theta = 60°$, $70°$, $80°$, and $90°$ at fixed $v_0/v_{\rm A} = 12$. Figure 8 shows the same quantities in Fig. 7, except that x-axis is θ. According to the 1D theoretical and simulation study [8], as θ decreases from 90°, it takes longer for a strong magnetic-field pulse to split into two pulses. The 2D simulation, as shown in Fig. 8 (a), confirms this, where $t_{\rm spl}$ is plotted as a function of θ. The amplitudes of $\bar{B}_z$ and 2D fluctuation $\sigma_{\rm B}$ at $t = t_{\rm spl}$ are shown in Figs. 8 (b) and 8 (c), indicating that these values are almost constant with θ. The wavenumbers k_z of the dominant mode of δB_z at $t = t_{\rm spl}$, which are plotted in Fig. 8 (d), are roughly estimated as $ck/\omega_{\rm pe} \sim 0.2$ for all the θ's. For the generated forward and reverse shock waves, the values of $M_{\rm fm}$, $B_{\rm m}$, $\sigma_{\rm B}$, and k_z averaged over the period after $t = t_{\rm spl}$ are almost constant with θ.

5. Summary

We have studied the interactions between exploding and surrounding plasmas in an external magnetic field using a 2D electromagnetic particle code with full ion and electron dynamics. After the exploding ions penetrate the surrounding plasma, a strong magnetic field pulse forms near the front of the exploding plasma. Because of the modified two-stream instabilities, 2D electromagnetic fluctuations grow to large amplitudes in this pulse. At $\Omega_i t \simeq 1$,

the pulse starts to split into two pulses, which then develop into forward and reverse shock waves. We performed simulations for various values of the initial velocity of the exploding plasma and of the angle between the velocity and external magnetic field. We then discussed the parametric dependence of the time for a strong magnetic-field pulse to split into two, the amplitudes of the generated pulses, and the properties of 2D magnetic fluctuations.

Acknowledgement

This work was carried out by the collaboration program Grant Nos. NIFS12KNSS036 and NIFS12KNXN246 of the National Institute for Fusion Science and by the joint research program of the Solar-Terrestrial Environment Laboratory, Nagoya University. It was also supported in part by a Grant-in-Aid for Scientific Research (C) Grant No. 24540535 of Japan Society for the Promotion of Science.

[1] L. Spitzer, *Physical Processes in the Interstellar Medium* (Wiley-Interscience, New York, 1978).
[2] D.A. Tidman and N.A. Krall, *Shock Waves in Collisionless Plasmas* (Wiley-Interscience, New York, 1971).
[3] K. Yamauchi and Y. Ohsawa, Phys. Plasmas **14**, 053110 (2007).
[4] M. Toida and T. Uragami, Phys. Plasmas **20**, 112302 (2013).
[5] N.A. Krall and P.C. Liewer, Phys. Rev. A **4**, 2094 (1971).
[6] J.B. McBride, E. Ott, J.P. Boris and J.H. Orens, Phys. Fluids **15**, 2367 (1972).
[7] C.S. Wu, Y.M. Zhou, S.T. Tsai, S.C. Guo, D. Winske and K. Papadopoulos, Phys. Fluids **26**, 1259 (1983).
[8] K. Yamauchi and Y. Ohsawa, J. Phys. Soc. Jpn. **77**, 054501 (2008).